The 2010 IEEE/RSJ International Conference on
Intelligent Robots and Systems
October 18-22, 2010, Taipei, Taiwan

Deformation Path Planning for Manipulation of Flexible Circuit Boards

Yuya Asano, Hidefumi Wakamatsu Eiji Morinaga, Eiji Arai and Shinichi Hirai

***Abstract*—A differential geometry based modeling of a belt object to represent its deformation path is proposed. Adequate deformation path of a belt object such as film circuit boards or flexible circuit boards must be generated for automatic manipulation and assembly. First, deformation of a belt object is described using the curvature of its central axis, torsion around the central axis and the curvature in the transverse direction. Second, a method to derive an adequate transition of the object shape from the initial state to the final state is proposed. It can be derived by minimizing the maximum of the local potential energy in the belt object during its manipulation. This is because locally excessive potential energy often leads to the excessive stress that makes fractures in the belt object. Finally, the validity of our proposed deformation path is verified by estimating the maximum local potential energy in a belt object.**

I. Introduction

DUE to downsizing of various electronic devices such as notebook PCs, mobile phones, digital cameras, and so on, more film circuit boards or flexible circuit boards illustrated in Fig.1 are used instead of conventional hard circuit board. It is difficult to assemble such flexible boards by a robot because they can be easily deformed during their manipulation process and they must be deform in the final state. For example, the flexible circuit board shown in Fig.1-(a) must deform to the objective shape illustrated in Fig.1-(b) to install into the hinge part of a flip phone. Therefore, analysis and estimation of film/flexible circuit boards is required.

In computer graphics, a deformable object is represented by a set of particles connected by mechanical elements [1]. Recently, fast algorithms have been introduced to describe liner object deformation using Cosserat formulation [2]. Cosserat elements possess six degrees of freedom; three for translation displacement and three for rotational displacement. Flexure, torsion, and extension of a liner object can be described by use of Cosserat elements. In robotics, insertion of a wire into a hole in 2D space has been analyzed using a beam model of the wire to derive a strategy to perform the insertion successfully [3][4]. Kosuge et al. have proposed a control algorithm of dual manipulators handling flexible sheet metal [5]. Lamiraux et al. have proposed a method of path planning for elastic object manipulation with its deformation to avoid contact with obstacles in a static environment [6]. Saha and Isto proposed a motion planner for manipulating ropes and realized tying several knots using two cooperating robot arms [7]. In differential geometry, curved lines in 2D or 3D space have been studied to describe their shapes mathematically [8]. Moll et al. have proposed a method to compute the stable shape of a liner object under some geometrical constraints quickly based on differential geometry [9]. It can be applied to path planning for flexible wires. Jian proposed the modeling method for deformable shell-liked object [10].

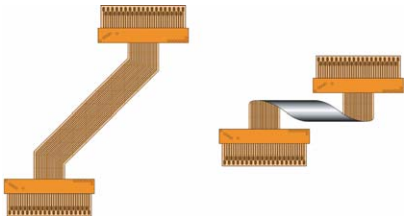

(a) Natural shape (b) Objective shape

Fig. 1. Example of flexible circuit board

As above, the modeling method to represent the object deformation and the method to manipulate it has been proposed. However, to my knowledge, there is not a research to estimate the deformed shape and load condition of it during its manipulation process. A flexible circuit board is a deformable object. So, it is possible to be deformed to contact with itself or obstacles in a static environment. In addition, a flexible circuit board is precision mechanical equipment. This means that it is possible to make fracture when it is deformed largely during its manipulation process. It can be easily bent along the central axis, but it must not be twisted around the central axis because it may cause the crack at the transverse edges leading to wiring disconnection. So, it is required to estimate the deformation shape and load condition of the object during its manipulation process.

In solid mechanics, the Kirchhoff theory for thin plates and Reissner-Mindlin theory for thick plates have been used [11]. For extremely thin plates, the inextensional theory was proposed [12]. In this theory, it is assumed that the middle surface of a plate is inextensional, that is, the surface of the plate is developable. Based on these theories, the deformed shape and load condition of the object can be calculated using the Finite Element Method (FEM). However, the high aspect ratio of thin objects often causes instability in computation of deformed shapes. Wakamatsu has proposed a differential geometry to represent linear object deformations and path planning [13]. In this paper, we apply this theory to deformation and deformation path of a belt object.

Y. Asano, H. Wakamatsu, E. Morinaga and E. Arai are with Dept. of Materials & Manufacturing Science, Graduate School of Eng., Osaka Univ., 2-1 Yamadaoka, Suita, Osaka 565-0871, Japan {y-asano, wakamatu, morinaga, arai}@mapse.eng.osaka-u.ac.jp

S. Hirai is with Dept. of Robotics., Ritsumeikan Univ., 1-1-1 Noji Higashi, Kusatsu, Shiga 525-8577, Japan hirai@se.ritsumei.ac.jp

II. DEFORMATION MODELING OF A BELT OBJECT

Description of deformed surface

It is assumed that the belt object is l long, b wide and h thick. Let u be the distance from one end of a belt object along the central axis in its longitudinal direction and v be the distance from the central axis in the transverse direction of the object. Let P(u, v) be a point on the object. In order to describe deformation of the central axis of a belt object, the global space coordinate system and the local object coordinate systems at individual points on the object are introduced as shown in Fig.2. Let O-xyz be the coordinate system fixed in space and P-$\xi\eta\zeta$ be the coordinate system fixed at an arbitrary point P(u, 0) on the central axis of the object. Select the direction of coordinates so that the ξ-, η-, and ζ-axis are parallel to the x-, y-, and z-axes, respectively, in the natural state. Deformation of the central axis is then represented by the relationship between the local coordinate system P- $\xi\eta\zeta$ at each point on the object and the global coordinate system O-xyz. Let$\boldsymbol{\xi}$, $\boldsymbol{\eta}$, and $\boldsymbol{\zeta}$ be unit vector along the ξ-, η-, and ζ-axes, respectively, at any point P (u, 0). By analogy with angular velocities of a rigid object, partial differentiation of these unit vector with respect to u are described by

$$\frac{d}{du}\begin{bmatrix}\boldsymbol{\xi} & \boldsymbol{\eta} & \boldsymbol{\zeta}\end{bmatrix}=\begin{bmatrix}\boldsymbol{\xi} & \boldsymbol{\eta} & \boldsymbol{\zeta}\end{bmatrix}\begin{bmatrix}0 & -\omega_\zeta & \omega_\eta\\ \omega_\zeta & 0 & -\omega_\xi\\ -\omega_\eta & \omega_\xi & 0\end{bmatrix} \tag{1}$$

where ω_ξ, ω_η, and ω_ζ are infinitesimal ratios of rotation angles around the ξ-, η-, and ζ-axes, respectively, at point P(u, 0). Note that ω_ξ and ω_ζ correspond to curvatures of central axis in the $\eta\zeta$-plane and in the $\xi\eta$-plane respectively, and ω_η correspond to torsional ratio around the central axis. Solving differential equations described by eq.(1) numerically, vector $\boldsymbol{\xi}$, $\boldsymbol{\eta}$, and $\boldsymbol{\zeta}$ at point P(u,0) can be determined. Let $\boldsymbol{x}$ be the position vector at P(u, 0). The position vector can be computed by integrating vector $\boldsymbol{\eta}$(u, 0). Namely,

$$\boldsymbol{x}(u,0)=\boldsymbol{x}_0+\int_0^u\boldsymbol{\eta}(u,0)du \tag{2}$$

where $\boldsymbol{x_0}=[x_0 \quad y_0 \quad z_0]^{\mathrm{T}}$ is the position vector at the end point P(0, 0). Here, we introduce parameter $\delta(u,v)$. It corresponds to the curvature in the transverse direction.

In this paper, it is assumed that four parameters $\omega_\xi(u,0)$, $\omega_\eta(u,0)$, $\omega_\zeta(u,0)$ and $\delta(u,0)$ are constant with respect to v because the width of the belt object is sufficiently smaller than its length, namely,

$$\left.\begin{aligned}\omega_\xi(u,v)&=\omega_\xi(u,0)\\ \omega_\eta(u,v)&=\omega_\eta(u,0)\\ \omega_\zeta(u,v)&=\omega_\zeta(u,0)\\ \delta(u,v)&=\delta(u,0)\end{aligned}\right\}\forall v\in\left[-\frac{b}{2},\frac{b}{2}\right]. \tag{3}$$

Thus, the shape of a belt object can be represented with the spine curve corresponding to the central axis and ribs describing curvature in the transverse direction at each point on the spine. This model is referred to as "*snake-bone*" model in this paper.

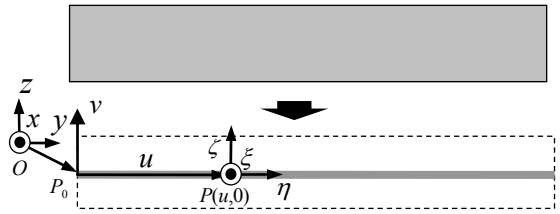

Fig. 2. Coordinate of belt object

Potential energy and geometric constraint

Let us formulate the potential energy of a deformed belt object. We can formulate the potential energy of a belt object with Kirchhoff theory as follows:

$$\begin{aligned}U=&\frac{E}{2(1-\upsilon^2)}\frac{bh^3}{12}\int_0^l\left(\kappa_\eta^2+\kappa_\zeta^2+2\upsilon\kappa_\eta\kappa_\zeta\right)du+\frac{G}{2}\frac{bh^3}{3}\int_0^l\kappa_{\eta\zeta}^2du\\&+\frac{E}{2(1-\upsilon^2)}\frac{b^3h}{12}\int_0^l\kappa_\xi^2du\end{aligned} \tag{4}$$

where E, G and υ represent Young's modulus, modulus of rigidity and Poisson ratio, respectively. κ_ξ, κ_η, κ_ζ, and $\kappa_{\eta\zeta}$ are curvature in ξ-direction, η-direction, ζ-direction and torsional ratio around η-axis. These correspond to ω_ξ, $-\omega_\zeta$, δ, and ω_η respectively. So, Eq. (4) is described by

$$\begin{aligned}U=&\frac{E}{2(1-\upsilon^2)}\frac{bh^3}{12}\int_0^l\left(\omega_\zeta^2+\delta^2-2\upsilon\omega_\zeta\delta\right)du+\frac{G}{2}\frac{bh^3}{3}\int_0^l\omega_\eta^2du.\\&+\frac{E}{2(1-\upsilon^2)}\frac{b^3h}{12}\int_0^l\omega_\xi^2du.\end{aligned} \tag{5}$$

Next, let us formulate geometric constraints imposed on a belt object. Let $\boldsymbol{l}=[l_x \quad l_y \quad l_z]^T$ be a predetermined vector describing the relative position between two operational points on the central axis of a belt object, $\boldsymbol{x}$ (u_a) and $\boldsymbol{x}$ (u_b). Recall that the spatial coordinates corresponding to distance u are given by Eq.(2). Thus, the following equation must be satisfied:

$$\boldsymbol{x}(u_b)-\boldsymbol{x}(u_a)=\boldsymbol{l}. \tag{6}$$

The orientational constraint at operation point $\boldsymbol{P}$ (u_c) is simply described as follows:

$$\boldsymbol{\xi}(u_c)=\boldsymbol{\xi}_c,\quad \boldsymbol{\eta}(u_c)=\boldsymbol{\eta}_c,\quad \boldsymbol{\zeta}(u_c)=\boldsymbol{\zeta}_c \tag{7}$$

where $\boldsymbol{\xi}_c$, $\boldsymbol{\eta}_c$ and $\boldsymbol{\zeta}_c$ are predefined unit vectors at this point. Therefore, the shape of a belt object is determined by minimizing the potential energy described by Eq.(5) under geometric constraints imposed on the object described by Eqs.(6) and (7). Namely, computation of the deformed shape of the object results in variational problem under equation and inequality constraints.

In fishbone model proposed in [14], rotation around ξ-axis and torsion around the central axis without bending are prohibited to maintain developability of the surface described

by the following equations;

$$\left.\begin{array}{c}\omega_{\xi}=0\\ -\omega_{\zeta}\delta-\omega_{\eta}^{2}=0\end{array}\right\}\quad \forall u\in[0,l] \tag{8}$$

The former deformation causes normal stress σ_{η} and the latter deformation causes shearing stress $\tau_{\xi\zeta}$, which reach to their maximum at transverse edges. To prevent from cracking, these stresses must be estimated and evaluated. In our snake-bone model, they can be estimated because the developability of the object surface is not assumed. Therefore, snake-bone model is more suitable for representation and evaluation of belt object deformation.

Computational algorithm for belt object deformation

Wakamatsu developed an algorithm based on Ritz's method [15] and a nonlinear programming technique to compute linear object deformation. That algorithm can be applied to the computation of belt object deformation.

Let us express functions $\omega_{\xi}(u)$, $\omega_{\eta}(u)$, $\omega_{\zeta}(u)$ and $\delta(u)$ by linear combinations of basis functions $e_1(u)$ through $e_n(u)$:

$$\begin{aligned}\omega_{\xi}(u)&=\boldsymbol{a}^{\xi}\cdot\boldsymbol{e}(u),\quad \omega_{\eta}(u)=\boldsymbol{a}^{\eta}\cdot\boldsymbol{e}(u)\\ \omega_{\zeta}(u)&=\boldsymbol{a}^{\zeta}\cdot\boldsymbol{e}(u),\quad \delta(u)=\boldsymbol{a}^{\delta}\cdot\boldsymbol{e}(u)\end{aligned} \tag{9}$$

where $\boldsymbol{a}^{\xi}, \boldsymbol{a}^{\eta}, \boldsymbol{a}^{\zeta}$ and $\boldsymbol{a}^{\delta}$ are vectors consisting of coefficients corresponding to functions $\omega_{\xi}(u)$, $\omega_{\eta}(u)$, $\omega_{\zeta}(u)$ and $\delta(u)$ respectively, and vector $\boldsymbol{e}(u)$ is composed of basis functions $e_1(u)$ through $e_n(u)$. Substituting the above equation into Eq.(5), potential energy U is described by a function of coefficient vectors $\boldsymbol{a}^{\xi}$, $\boldsymbol{a}^{\eta}, \boldsymbol{a}^{\zeta}$ and $\boldsymbol{a}^{\delta}$. Constraints are also described by conditions involving the coefficient vectors. Consequently, the deformed shape of a belt object can be derived by computing a set of coefficient vectors $\boldsymbol{a}^{\xi}$, $\boldsymbol{a}^{\eta}, \boldsymbol{a}^{\zeta}$ and $\boldsymbol{a}^{\delta}$ that minimizes the potential energy under the constraints. The minimizing problem can be solved by use of a nonlinear programming technique such as multiplier method[16]. Let us compute the belt object deformation. The natural shape of a belt object is illustrated in Fig.3-(a). It is 200mm long, 20mm wide and 0.14mm thick. Positional and orientational constraints are shown in Fig.3-(b). Fig.4 shows the computational result. As shown in Fig.4, our proposed method can derive the deformed shape of a belt object bending and twisting continuously to satisfy given geometric constraints.

III. DEFORMATION PATH PLANNING FOR BELT OBJECT MANIPULATION

In manipulation of a deformable belt object, the object often deformed one shape into another. Let us determine desirable deformation path from an initial shape to a target shape. It is generally required to deform a belt object with little stress. Excessive potential energy of a belt object can be easily transformed into kinetic energy by a small disturbance force, in which case the shape of the object can become unstable and change dynamically. Thus, the potential energy

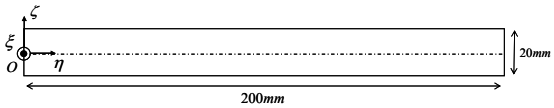

(a) Initial shape

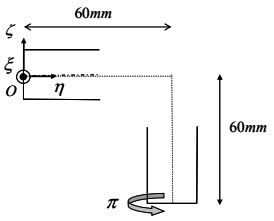

(b) Geometric constraint of the both ends

Fig. 3. Example of belt object deformation

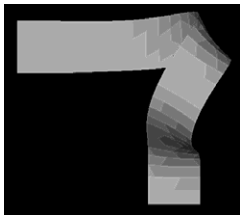

(a) Top view

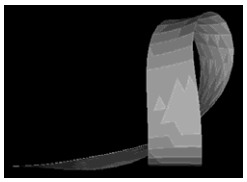

(b) Front view

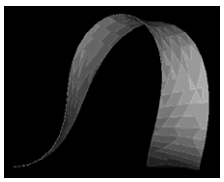

(c) Side view

Fig. 4. Computational result

of a belt object should be small during its deformation process. In [13], Wakamatsu has proposed the deformation path of a linear object that minimizes the value of the maximum potential energy of the object during its deformation path. However, as for the belt object such as flexible/film circuit board, while the whole potential energy is small, the local stress can be excessive during its manipulation process. For example, when a belt object bends around ξ-axis or twists around η-axis, the excessive stress can be occurred in the local area of the object. This excessive stress usually leads to fracture of the belt object because flexible/film circuit board is a precision mechanical equipment and easily can be broken. When we evaluate the damage of a belt object with the whole potential energy, the locally excessive stress can be applied to the belt object even if the whole potential energy is the small. So, it's not desirable to evaluate the damage of the belt object with its whole potential energy proposed in [13]. Thus, in this paper, we evaluate the damage of the belt object with its local

potential energy.

Recall that the deformation of a belt object can be described by coefficient vectors $\boldsymbol{a}^{\xi}, \boldsymbol{a}^{\eta}, \boldsymbol{a}^{\zeta}$ and $\boldsymbol{a}^{\delta}$ corresponding to $\omega_{\xi}(u)$, $\omega_{\eta}(u)$, $\omega_{\zeta}(u)$ and $\delta(u)$, respectively. Let $\boldsymbol{a}$ be a collective vector of these coefficients, namely

$$\boldsymbol{a} = \left[\boldsymbol{a}_{\xi} \quad \boldsymbol{a}_{\eta} \quad \boldsymbol{a}_{\zeta} \quad \boldsymbol{a}_{\delta}\right]^{T}. \tag{10}$$

One deformation corresponds to a point in coefficient space. The deformation process of a belt object is then given by a path in the coefficient space. Let $\boldsymbol{a}_0$ and $\boldsymbol{a}_1$ be the initial and goal deformations, respectively, and let $\boldsymbol{a}(k)$ $(0 \le k \le 1)$ be a path from the initial deformation to the goal deformation. Note that functions $(1-k), k, k^i(1-k)(i = 1,2,\ldots)$ and $k(1-k)^j(j = 1,2,\ldots)$ are a set of bases of a function space. Then, based on the Taylor expansion, any path can be approximated by a linear combination of these base functions

$$\boldsymbol{a}(\boldsymbol{b},k) = (1-k)\boldsymbol{a}_0 + k\boldsymbol{a}_1 + \sum_{i=1}^{\infty} \boldsymbol{b}_{i,0} k^i (1-k) + \sum_{j=1}^{\infty} \boldsymbol{b}_{j,1} k(1-k)^j \tag{11}$$

where $\boldsymbol{b}_{i,0}, \boldsymbol{b}_{j,1}$ are expansion coefficients. Any path can be represented by an infinite number of coefficients vectors: $\boldsymbol{b}_{i,0}, \boldsymbol{b}_{j,1}$. Let $\boldsymbol{b}$ be a collective vector consisting of these coefficient vectors, which are referred to as *the deformation path vector*. The deformation path vector $\boldsymbol{b}$ determines a deformation path from the initial deformation $\boldsymbol{a}(\boldsymbol{b},0) = \boldsymbol{a}_0$ to the goal deformation $\boldsymbol{a}(\boldsymbol{b},1) = \boldsymbol{a}_1$. Vectors $\boldsymbol{a}(\boldsymbol{b}, k)$ corresponds to an intermediate deformation along the path.

Let $U_{local}(\boldsymbol{b},k,u)$ be the local potential energy of an infinitesimal part being Δu long at point P(u) of the object with deformation $\boldsymbol{a}(\boldsymbol{b},k)$. It is described as follow:

$$U_{local}(\boldsymbol{b},k,u) = \frac{E}{2(1-\upsilon^2)} \frac{bh^3}{12} \left(\omega_{\zeta}^2 + \delta^2 - 2\upsilon\omega_{\zeta}\delta\right)\Delta u + \frac{G}{2}\frac{bh^3}{3}\omega_{\eta}^2 \Delta u + \frac{E}{2(1-\upsilon^2)} \frac{b^3 h}{12} \omega_{\xi}^2 \Delta u. \tag{12}$$

Let $U_{max}(\boldsymbol{b},k)$ be the maximum of the local potential energy of the object with deformation $\boldsymbol{a}(\boldsymbol{b},k)$. $U_{max}(\boldsymbol{b},k)$ is described as follow:

$$U_{max}(\boldsymbol{b},k) = \max_{0 \le u \le l} U_{local}(\boldsymbol{b},k,u). \tag{13}$$

In this paper, we evaluate the local potential energy of the belt object during its deformation process. We define the load condition W of the belt object along a deformation path as follow:

$$W(\boldsymbol{b}) = \int_0^l U_{\max}(\boldsymbol{b},k)dk. \tag{14}$$

Recall that geometric constraints imposed on an object can be described by a set of functions of vector $\boldsymbol{b}$. For example, when the relative position and orientation of the both end of the belt object is fixed during its deformation process, following equation must be satisfied:

$$\int_0^1 \left(\boldsymbol{x}(k,u_b) - \boldsymbol{x}(k,u_a) - \boldsymbol{l}\right)^2 dk = 0 \tag{15}$$

where, $\boldsymbol{l} = [l_x \quad l_y \quad l_z]^T$ is a predetermined vector describing the relative position between two operational points on the central axis of a belt object, $\boldsymbol{x}(k, u_a)$ and $\boldsymbol{x}(k, u_b)$.Consequently, it is found that the desirable deformation path can be derived by minimizing the function $W(\boldsymbol{b})$ under the geometric constraints.

IV. VERIFICATION OF PROPOSED METHOD

In this section, the validity of our proposed method will be verified. First, the simulated deformed shape will be experimentally verified by measuring the deformed shape of the belt object. Computation algorithm to derive the belt object shape was previously mentioned. In this paper, the number of coefficients were 16 for $\boldsymbol{a}^{\xi}$, $\boldsymbol{a}^{\eta}, \boldsymbol{a}^{\zeta}$ and $\boldsymbol{a}^{\delta}$, respectively, and 64 in all. In Eq.(9), the following set of basis functions were used in the computation:

$$\begin{aligned} &e_1 = 1, \quad e_2 = u, \\ &e_{2i+1} = \cos\frac{\pi i u}{U}, \quad e_{2i+2} = \sin\frac{\pi i u}{U}, \quad (i = 1,\ldots,7) \end{aligned} \tag{16}$$

To calculate unit vector ξ-, η-, and ζ-axis at point $\boldsymbol{x}(u)$ from Eq.(1), the Runge-Kutta method was used. Computation was performed on two 2.0GHz AMD Opteron 246 CPUs with 3GB memory operated by Solaris 10. Programs were compiled by a Sun C Compiler 5.8 with optimization option O5. It took about 10 minutes to compute.

We measured a belt-shaped flexible polystyrol sheets with a 3D scanner. It is 200mm long, 20mm wide, and 0.14mm thick. Both ends of the belt object illustrated in Fig.3-(a) are fixed as shown in Fig.5. Young's modulus E is 3.0GPa and Poisson ratio υ is 0.34. Fig.6 shows the computational result and the experimental result. . As shown in this figure, the computational result is quite coincident with the actual shape. Thus, our modeling method can estimate the deformation of a belt object.

Next, our proposed procedure to derive adequate deformation path is compared with that proposed in [13]. In this paper, the former is referred to as *the local energy evaluation* and the latter is referred to as *the whole energy evaluation*. Especially, we focus on the deformation path shape, the whole potential energy of it, the maximum local potential energy of it, and the maximum principal stress of it.

Both ends of the belt object illustrated in Fig.3-(a) are fixed as shown in Fig.5 and the object is deformed from the shape being convex upward to being convex downward.

In Eq.(11), we expand $\boldsymbol{a}(k)$ to the third order. Then, the deformation path vector $\boldsymbol{b}$ was the collective vector consisting of $\boldsymbol{b}_{1,0}, \boldsymbol{b}_{2,0}$ and $\boldsymbol{b}_{2,1}$. And the number of coefficient was 16 for $\boldsymbol{b}_{1,0}, \boldsymbol{b}_{2,0}, \boldsymbol{b}_{2,1}$, respectively. So, the number of coefficients were 48 for $\boldsymbol{a}^{\xi}$, $\boldsymbol{a}^{\eta}, \boldsymbol{a}^{\zeta}$ and $\boldsymbol{a}^{\delta}$ respectively and 192 in all. The basis functions were represented in Eq.(16). The optimal deformation path can be derived by minimizing the function $W(\boldsymbol{b})$ represented in Eq.(14) under the

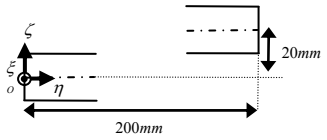

Fig. 5. Geometric constraint for both ends

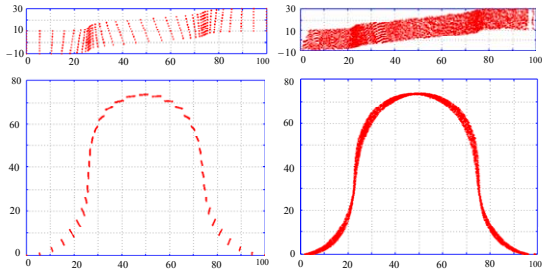

(a)Computational result (b)Experimental result

Fig. 6. Example of belt object deformation

geometric constraints described in Eq.(15). It took about 30 hours to compute. Fig.7 and Fig.8 show the computed deformation path. Fig.8 is obtained with the whole energy evaluation and Fig.9 is from the local energy evaluation, respectively. As shown in these figures, both deformation paths look similarly. Then, let us evaluate the load conditions of these deformation paths. Fig.9 and Fig.10 show the whole potential energy of deformed belt object during its deformation process and the maximum local potential energy of it, respectively. As shown in these figures, the whole potential energy of the local energy evaluation is larger than that of the whole energy evaluation. However, the maximum local energy is smaller than that. In addition, the maximum principal stress is also smaller as shown in table1. As for the manipulation of a flexible/film circuit board, the fracture happens at the point where the local potential energy is excessively large. In the local energy evaluation, larger stress is applied than that in the whole energy evaluation as for to the whole object, however, as for to the local area, smaller stress is applied in the local energy evaluation. So, the local energy evaluation is more suitable for derivation of optimal deformation path without crack or fracture of the belt object.

V. FUTURE WORKS

We proposed locally less stressed deformation path of a belt object. This deformation path can not be performed by controlling one end of a belt object. A set of control points may be needed to perform the optimal deformation path within a given margin of error. Feasibility can be examined by simulating a deformation path performed by the set of control points. However, considering the manipulation in the real production field, the manipulation is usually performed by one or two robot arms and control points should not be shifted one arm to the other. So, as future works, possibly less

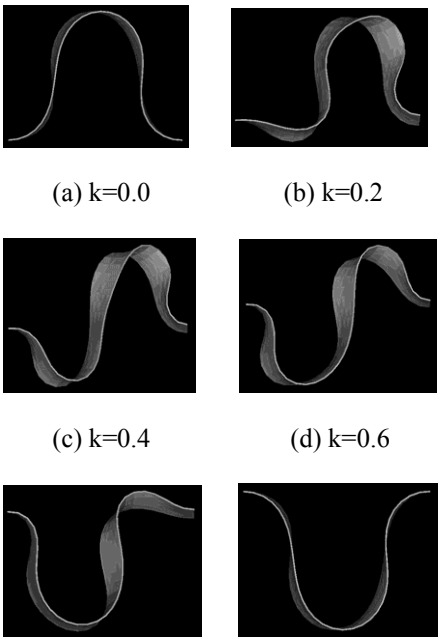

(a) k=0.0 (b) k=0.2

(c) k=0.4 (d) k=0.6

(e) k=0.8 (f)k=1.0

Fig. 7. Deformation path by the whole energy evaluation.

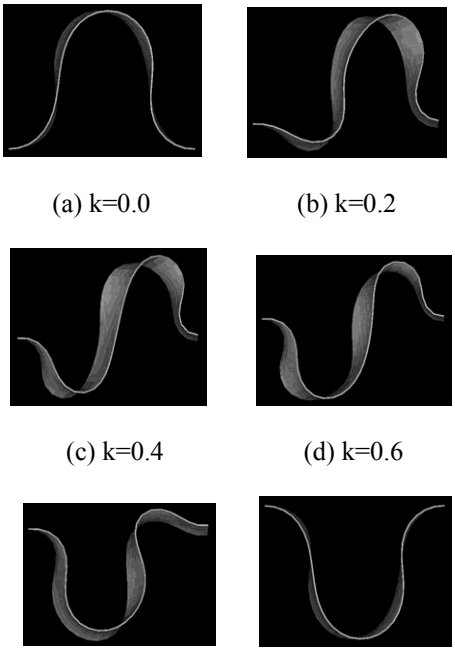

(a) k=0.0 (b) k=0.2

(c) k=0.4 (d) k=0.6

(e) k=0.8 (f)k=1.0

Fig. 8. Deformation path by the local energy evaluation.

control points and manipulation path should be calculated to approximately realize our proposed optimal deformation path.

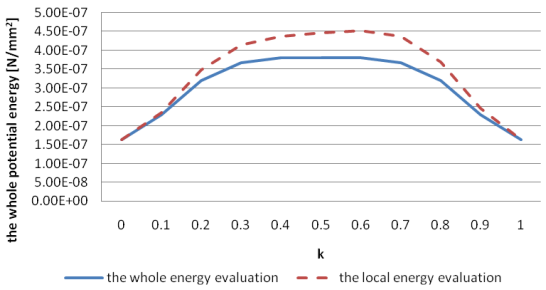

Fig. 9. The whole potential energy.

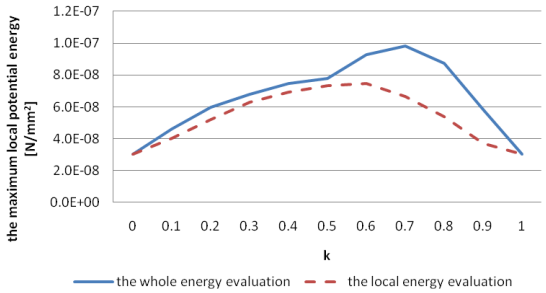

Fig. 10. The maximum local potential energy.

Table 1.The maximum principal stress

	The maximum principal stress [MPa]	k
The whole energy evaluation	37.9	0.7
The local energy evaluation	28.2	0.7

VI. CONCLUSION

A differential geometry based modeling to represent belt object deformation and optimal deformation path were proposed for manipulation of film/flexible circuit boards. First, the deformed shape of a belt object was represented as functions of four independent parameters. Then we estimated belt object deformation by optimizing these parameters so that potential energy of the object attains its minimum value under constraints imposed on it. Second, adequate deformation path of a belt object was derived by minimizing maximum local potential energy during its deformation process. Finally, the validity of the proposed model was verified by comparing the computed shape of a belt object with its measured shape. Furthermore, as for deformation path, we compared the deformation path proposed in this paper with that proposed in [13] in terms of the deformation shape, the whole potential energy, the maximum local potential energy, and the maximum principal stress of the object during its deformation process. The local potential energy and the maximum principal stress during our proposed deformation path are smaller than those proposed in [13] though they are more loaded as for the whole potential energy. Consequently, our proposed method can derive adequate deformation path, which prevents from making cracks.

REFERENCES

[1] A. Witkin and W. Welch, "Fast Animation and Control of Nonrigid Structures", *Computer Graphics*, Vol.24, 1990, pp. 224-252.

[2] D. k. Pai, "STANDS: Interactive Simulation of Thin Solids using Cosserat Models", *Computer Graphic Forum*, Vol.21, No.3, 2002, pp. 342-352.

[3] Y. E. Zheng, R. Pei, and C. Chen, "Strategies for Automatic Assembly of Deformable Objects", *Proc. of IEEE Int. Conf. Robotics and Automation*, pp. 2598-2603, 1991.

[4] H. Nakagaki, K. Kitagaki, and H. Tsukune, "Study of Insertion Task of a Flexible Beam into a Hole", *Proc. of IEEE Int. Conf. Robotics and Automation*, pp. 330-335, 1995.

[5] K. Kosuge, M. Sakaki, K. Kanitani, H. Yoshida, and T. Fukuda, "Manipulation of a Flexible Object by Dual Manipulators", *Proc. of IEEE Int. Conf. Robotics and Automation*, pp.188-208, 1995.

[6] F. Lamiraux and L. E. Kravaki, "Planning Paths for Elastic Objects under Manipulation Constraints", *Int, J. Robotics Research*, Vol.20, No.3, pp. 188-208, 2001.

[7] M. Saha and P. Isto, "Manipulation Planning for Deformable Linear Objects", *J. IEEE Transactions on Robotics*, Vol.23, No.6, pp. 1141-1150, 2007.

[8] A.Gray, *Modern Differential Geometry of Curves and Surfance*, CRC Press, 1993.

[9] M. Moll and L. E. Kravraki, "Path Planning for variable Resolution Minimal-Energy Curves of Constant Length", *Proc. of IEEE Int. Conf. Robotic and Automation*, pp. 2142-2147, 2005.

[10] J. Tian and Y. B. jia "Modeling Deformable Shell-like Objects Grasped by a Robot Hand", *IEEE International Conference on Robotics and Automation*, pp. 1297-1302, 2009.

[11] S. Timoshenko, *Theory of Plates and Shells*, McGraw-Hill Book Company, Inc., 1940.

[12] E. H. Mansfield, "The Inextensional Theory for Thin Flat Plates", *The Quarterly J. Mechanics and Applied Mathematics*, Vol.8, pp. 338-352, 1955.

[13] H. Wakamatsu and S. Hirai, "Static Modeling of Linear Object Deformation based on Differential Geometry", *International Journal of Robotics Research*, Vol.23, No.3, March, pp. 293-311, 2004.

[14] H. Wakamatsu, E. Arai, and S. Hirai. "Fishbone Model for Belt Object Deformation", *Robotics: Science and Systems*Ш, The MIT Press, pp. 88-96, 2008.

[15] L. E. Elsgolc, *Calculus of Variations*, Pergamon Press, 1961.

[16] M. Avriel, *Nonlinear Programming: Analysis and Methods*, PreticeHall, 1976.